Interestingly, when the tractors of the 1/10-scale models with the roof differential were provided with well-rounded noses, the effect of gap previously observed only at high Reynolds number, with the sharp-edged tractor, was now observed at low Reynolds number. It seems to me that this can be explained by the fact that the sharp-edged tractor gave such a tremendous flow separation at low Reynolds numbers that the difference in air gap had no effect. The point of flow reattachment was downstream of the trailer face.

In later low-Reynolds-number tests with sharp-edged tractor configurations we found that drag reducing devices mounted to the tractor roof, such as the Rudkin-Wiley Airshield™ and the General Motors Dragfoiler™, had *no* influence. However, with the well-rounded nose on the tractor, the drag reductions *were* similar to those reported at higher Reynolds numbers during the Symposium. Subsequently, with a 1/2-scale model test at MIRA we experienced almost exactly the same performance as other investigators.

A. E. Perry

I have a comment which relates to the surface flow patterns you showed on Figs. 7a and 7b. I think that the patterns are very revealing. More work like that should be done on bluff bodies. If you look at the patterns carefully, you can see that they're full of singularities such as saddles and nodes. These are carefully classified in Lighthill's section of Rosenhead's book* on Laminar Boundary Layers.

Rosenhead, L., Editor (1963), Laminar Boundary Layers, Oxford University Press, pp. 72-82.

INTERACTION EFFECTS ON THE DRAG OF BLUFF BODIES IN TANDEM

A. ROSHKO and K. KOENIG

California Institute of Technology, Pasadena, California

ABSTRACT

The objective of this study is to obtain better understanding of the flow over two tandemly positioned bluff bodies in close enough proximity to strongly interact with each other. This interaction is often beneficial in that the drag of the overall system is reduced. Prototypes for this problem come from tractor-trailer and cab-van combinations, and from various add-on devices designed to reduce their drag.

The primary object of the present investigation is an axisymmetric configuration which seems to have first been studied by Saunders (1966). A disc of diameter d_1 is coaxially placed in front of a flat-faced cylinder of diameter d_2. For a given ratio d_1/d_2, there is a value of gap ratio, g^*/d_2, for which the drag of the forebody system is a minimum. In the most optimum configuration, $d_1/d_2 = 0.75$, $g^*/d_2 = 0.375$, and the corresponding forebody drag coefficient is 0.02, a remarkable reduction from the value of 0.75 for the cylinder alone. For each value of d_1/d_2, the minimum drag configuration, g^*/d_2, appears to correspond to a minimum dissipation condition in which the separation stream surface just matches (joins tangentially onto) the rearbody. Support for this idea is furnished by comparison with some results derived from free-streamline theory and from flow visualization experiments. However, when g^*/d_2 exceeds a critical value of about 0.5, the value of C_{Dmin} is almost an order of magnitude higher than for subcritical optimum gap ratios. The increase seems to be connected with the onset of cavity oscillations.

For non-axisymmetric geometry (square cross-sections) the separation surface cannot exactly match the rearbody and the subcritical minimum values of drag are higher than for circular cross-sections.

References p. 273.

NOTATION

A_1, A_2	frontal area of frontbody and rear body, respectively
C_D	drag coefficient of forebody system based on A_2 and freestream dynamic pressure
C_{Dmin}	minimum drag coefficient for fixed A_1/A_2
C_{D_1}	drag coefficient of frontbody based on A_1
$C_{D_{1_f}}$	drag coefficient of frontbody face based on A_1
C_{D_2}	drag coefficient of rearbody face based on A_2
C_p	local rearbody-face pressure coefficient
C_{p_s}	constant-pressure surface or free-streamline pressure coefficient
$C_p{}^*$	average cavity-pressure coefficient at optimum gap
d_1, d_2	diameter of frontbody and rearbody, respectively
$(d_1/d_2)_{cr}$	frontbody to rearbody diameter ratio at critical g^*/D_2
g	gap between frontbody and face of rearbody
g^*	optimum gap for a given d_1/d_2
$(g^*/d_2)_{cr}$	optimum gap ratio of critical geometry
q_∞	freestream dynamic pressure
r	radius of corner on rearbody face
$r_s(x)$	radial position of the separation surface
Re	Reynolds number based on q_∞ and d_2
τ_s	shear stress on separation surface
U_s	flow velocity outside separation surface
U_∞	freestream velocity

x coordinate parallel to freestream velocity

y radial location on rearbody face

INTRODUCTION

In analyses of the problem of reducing the drag of trucks and, especially, of tractor-trailers, the importance of the front end of the vehicle is always apparent. How to shape the cab and trailer to reduce overall drag, taking into account their mutual interaction, is an important question. The invention of devices to deflect and guide the flow from the tractor over the trailer has demonstrated that beneficial interference between otherwise high-drag bodies can be obtained. The technique of drafting used in automobile racing (described by Mr. Bobby Allison at this Symposium) provides another example of beneficial interference.

We thought it would be interesting and useful to investigate interference between bluff bodies of much simpler geometry than those of real road vehicles, the objective being to identify drag mechanisms and to better understand the conditions that lead to drag reduction of the system. We concluded that an *axisymmetric* configuration would have the needed simplicity and would also better represent the vehicle problem than would a two-dimensional one, and we were thus led to study the configuration shown in Fig. 1.

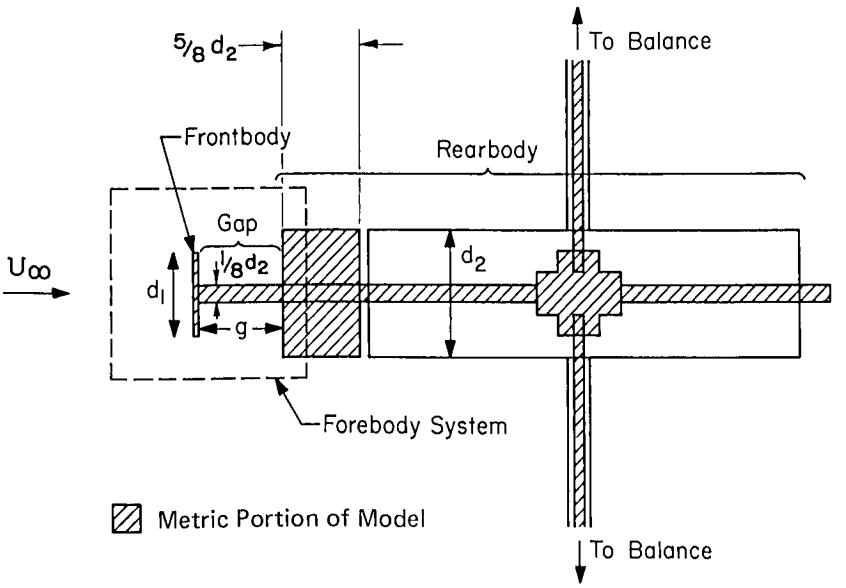

Fig. 1. Experimental model

References p. 273.

The object here is to investigate the drag of a semi-infinite half body, in this case a circular cylinder with a flat face. In *potential* flow the integral of the pressure over the area of this face is zero; in the *real* flow, separation from the edge leads to loss of the high suction near the edge and results in a face pressure drag whose coefficient $C_D \cong 0.75$, based on the cylinder's cross-sectional area. This is comparable to the drag coefficient of the front of a trailer without a tractor. If now a disc is placed coaxially in front of the cylinder, the pressure and thus the drag of the cylinder will be modified. In turn, the drag of the disc will be altered from the free body value of $C_D = 1.2$, Hoerner (1965), based on its own area. Denoting the disc and the face of the cylinder by subscripts 1 and 2, respectively, the total drag of the forebody *system* (frontbody and face of the rearbody) will be

$$D = D_1 + D_2 = (C_{D_1} A_1 + C_{D_2} A_2)\, q_\infty \tag{1}$$

where A_1 and A_2 are the respective cross-sectional areas, and q_∞ is the freestream dynamic pressure. In what follows, the drag coefficient for the system will be based on A_2, i.e.

$$C_D = \frac{D}{q_\infty A_2} \tag{2}$$

A configuration similar to this was investigated by Saunders (1966). His results, described briefly in his patent application, showed how the drag of the system can be minimized by suitable choice of diameter ratio d_1/d_2 and gap ratio g/d_2. The system in Saunder's experiments included all of the rearbody, i.e. its base pressure drag as well as skin friction on the sides, in addition to the frontbody. In our experiment we arranged to exclude the sides and base of the rearbody from the drag system by suspending only a short section of the front portion of the rearbody from the drag balance, as shown in Fig. 1. The pressure distribution in the slot between this active front section and the dummy part of the cylinder could be measured in order to correct for contributions to drag from the model internal pressure. These pressures were observed to depend in a consistent manner on the drag of the forebody system, i.e. C_p became more negative as C_D increased. Skin friction on the sides of the small active segment of the rearbody could contribute no more than 0.01 to C_D. (Measurements on a similar segment, but with a well-rounded leading edge to restore the edge suction, gave values of C_D less than 0.01 when tested without a frontbody.) With the forebody system isolated this way, the interaction effects are revealed much more clearly than when measurements are made on the complete system.

EXPERIMENTAL DETAILS

The configuration shown in Fig. 1 was built with d_2 = 8 in. (20.3 cm) for installation in the GALCIT* Merrill Wind Tunnel which has a test section 32 in. x 46 in. (81 cm x 117 cm) in cross-section and 104 in. (264 cm) long. The central sting supporting the forebody system was mounted on a unique force balance which had been designed and built by Professor F. Clauser, providing direct analog readout of the three aerodynamic forces and the three moments acting on the metric part of the model. This balance has an effective time constant of approximately 1 second. C_D repeatability for these experiments was approximately $\pm$ 0.006. Pressure distributions on the face of the rearbody and in the slot between the metric and dummy portions of the model were measured using 1/32 in. (0.08 cm) pressure orifices and a 0-100 mm Hg Barocel pressure transducer. Tygon tubing used to transmit the pressures and the Barocel gave a frequency response of approximately 17 Hz. The pressures were measured on a Hewlett-Packard Timer-Counter DVM with a variable integration time up to 10 seconds. Measurements were made at speeds from 25 to 190 ft/sec (7.6 to 57.9 m/sec); corresponding values of the Reynolds number, Re, based on d_2 were from 1 x 10^5 to 8 x 10^5.

The model could also be arranged so that only the frontbody was connected to the balance, all of the rearbody then becoming nonmetric. This permitted decomposition of the forebody system drag into contributions from the frontbody and the face of the rearbody.

A second model, with d_2 = 4 in. (10.2 cm), was built for installation in the GALCIT Free Surface Water Tunnel, Ward (1976), mainly for flow visualization with dye. The dye, diluted food coloring, was injected into the flow from the face of the frontbody, the face of the rearbody, or from an upstream probe, allowing the flow field to then be observed and photographed. These tests were made at a water speed of 3.5 ft/sec (1.1m/sec) giving a Reynolds number of 1 x 10^5.

In addition to the models with circular cross-section, cylinders of square cross-section were also constructed and tested in both facilities, the discs in front now being replaced by square plates.

RESULTS FOR CIRCULAR CROSS-SECTION

Measurements of the drag of the forebody system are shown in Fig. 2 for several frontbody-to-rearbody diameter ratios, with the gap ratio g/d_2 as the independent variable. Most remarkable is the great reduction in drag that can be achieved for certain combinations of d_1/d_2 and g/d_2. In particular, for $d_1/d_2 = 0.75$ the value of C_D is only 0.02 for $g/d_2 = 0.38$, compared to a value of about 0.75 for g = 0. This value is hardly higher than what could be achieved for a well shaped solid forebody system without separation. It is so low that its accuracy of measurement is perhaps no

* *Graduate Aeronautical Laboratories, California Institute of Technology.*

References p. 273.

better than ±30 percent. Minima are also reached for other values of d_1/d_2, even for $d_1/d_2 = 1.0$ whose minimum occurs at $g/d_2 = 1.5$. For $g/d_2 \to 0$, C_D tends to the value for the front face drag of the rearbody, namely 0.75; for $g/d_2 \to \infty$, the drag ought to approach the sum of the free field values of each body, i.e. using (1) and (2)

$$C_D \to C_{D_2} + C_{D_1} \left(\frac{d_1}{d_2}\right)^2 \cong 0.75 + 1.2\left(\frac{d_1}{d_2}\right)^2 \tag{3}$$

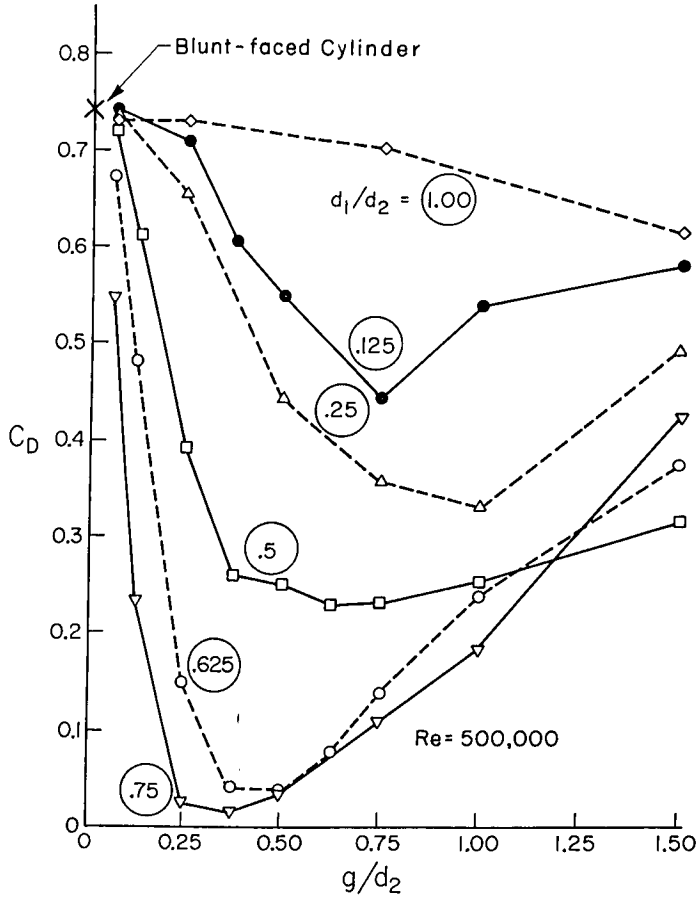

Fig. 2. Effect of gap on system drag (axisymmetric).

Fig. 3 shows some pictures obtained with dye visualization in the water tunnel. The exposure time for these photographs was 1/1000 sec. First, as a baseline for comparison, the rear cylinder without the front disc or its sting support is shown in Fig. 3a. The large separation from the edges accounts for the high value of $C_D \cong 0.75$. By contrast, in Fig. 3b is shown the configuration corresponding to $C_D = 0.03$, not quite optimum, while Fig. 3c shows the flow corresponding to the minimum value, $C_D \cong 0.02$, for this d_1/d_2. In both (b) and (c) it may be seen that the separation surface from the disc joins smoothly onto the edge of the rearbody, becoming a boundary layer on that body. Curiously, for the optimum case (c), the separation surface does not appear to join on quite as smoothly as in (b); there is a small overshoot before the point of reattachment. These minute details of the flow may be due to Reynolds number effects, however.

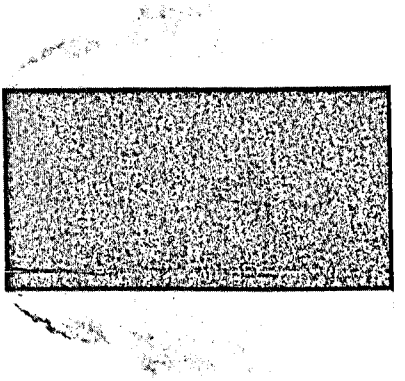

Fig. 3a. Blunt-faced cylinder. The perfect symmetry is the result of this picture being a composite. $C_D = 0.75$.

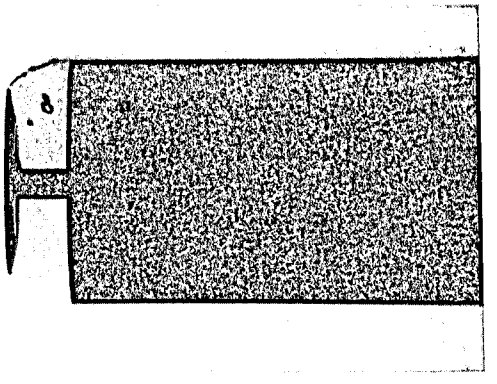

Fig. 3b. $d_1/d_2 = 0.75$, $g/d_2 = 0.25$, $C_D = 0.03$.

References p. 273.

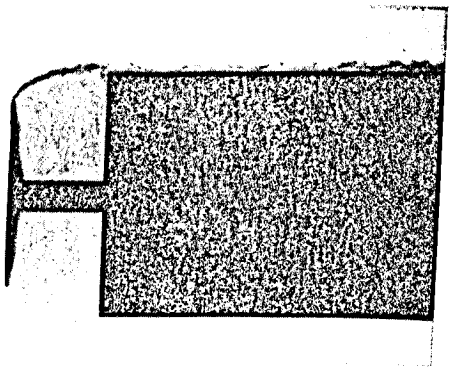

Fig. 3c. $d_1/d_2 = 0.75$, $g/d_2 = 0.375$, $C_D = 0.02$.

Figs. 3d and 3e show flows for which the gap is too small and too large, respectively, for optimum drag reduction; the values of C_D are 0.24 and 0.18.

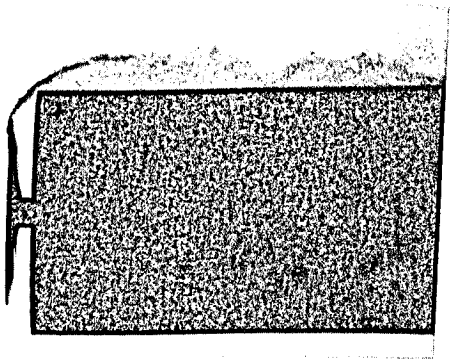

Fig. 3d. $d_1/d_2 = 0.75$, $g/d_2 = 0.125$, $C_D = 0.24$.

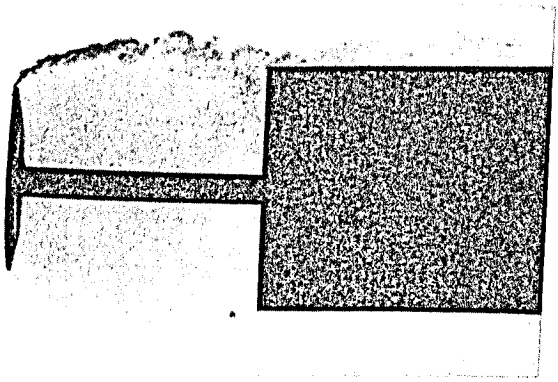

Fig. 3e. $d_1/d_2 = 0.75$, $g/d_2 = 1.0$, $C_D = 0.18$.

SOME THEORETICAL CONSIDERATIONS

As has been noted by Saunders (1966) and is evident from the flow pictures, favorable interference and low total drag occur when the separated flow from the frontbody, i.e. the separation stream surface, joins smoothly (in some sense) onto the front edge of the rearbody, so that the total extent of the separation region in the gap and beyond is minimized. Assuming that the separation surface is nearly a constant-pressure surface, a free-streamline analytical model can be used to calculate the gap corresponding to the condition of smooth flow onto the rearbody. In the free-streamline model, this is simply the downstream distance at which the separated stream surface becomes parallel to the freestream, i.e. tangent to the side of the rearbody, as shown in the inset sketch in Fig. 4. The free-streamline model can be analytically formulated in two-dimensional flow with the help of conformal mapping (Roshko, 1954), but for the axisymmetric case the computations have to be carried out numerically (Strück, 1970).

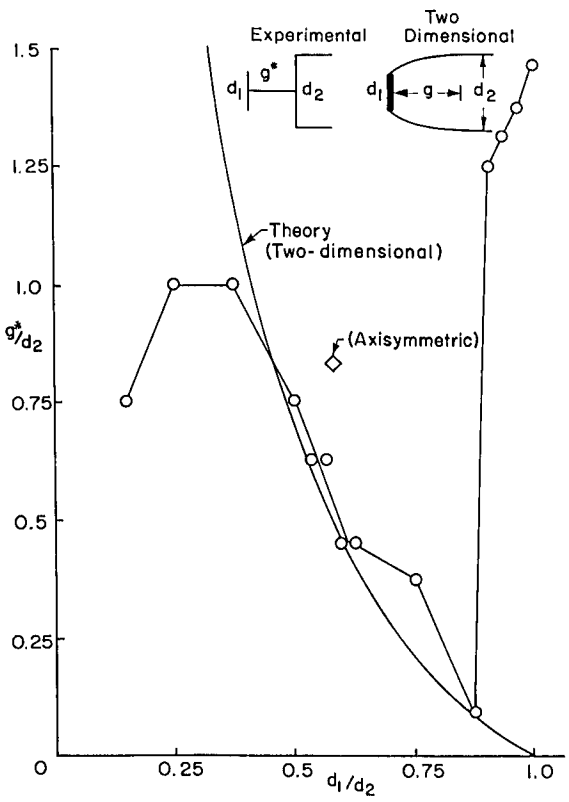

Fig. 4. Optimum gap.

References p. 273.

Shown in Fig. 4 are the results of the two-dimensional theory in the form of consistent combinations of gap and height ratio for a constant-pressure streamline joining tangentially onto the rearbody. The parameter varied to trace out the curve is the pressure coefficient on the constant-pressure separation stream surface (which is the same as the base pressure coefficient of the disc because the separated region is assumed to be a quiescent, constant-pressure region). The one computed case from Strück's work is also shown for comparison with the two-dimensional case. Also shown are our experimental values of g^*/d_2 for each value of d_1/d_2. These are taken from Fig. 2 where it may be seen that there is some uncertainty in determining precisely the value of g/d_2 for which minimum C_D occurs. The favorable comparison between the measured and calculated gap ratios over the range $0.38 < d_1/d_2 < 0.88$ suggests that the separated flow pattern for minimum drag corresponds fairly well with a free-streamline model. For values of d_1/d_2 closer to unity, the good correspondence does not hold up because the pressure coefficient on the separation streamline would be tending to negatively infinite values. For values of d_1/d_2 less than 0.38 the minimum values of C_D occur at values of gap width considerably smaller than for the free-streamline model. This is because, for larger gaps, the separation surface begins to close itself ahead of the rearbody and the flow field is quite different from that which is modeled by the free-streamline theory.

Some other results from the free-streamline analytical model may also be used for comparison with our experimental results. In particular, the free-streamline constant pressure associated with each d_1/d_2 can be compared to the measured pressure in the gap between the two bodies of our test configuration. To use the two-dimensional analytical result would be greatly in error; the axisymmetric result is the appropriate one and it can be estimated semi-empirically, as follows, without resort to the complete numerical calculation.

Temporarily regarding the free stream surface as a solid surface, the semi-infinite half body so defined has zero drag in potential flow, i.e.

$$D = D_{1_f} + D_s = 0 \tag{4}$$

where D_{1f} and D_s are the contributions from the front of the disc and from the constant-pressure surface, respectively, and $D_{1f} = C_{D1f} q_\infty A_1$ while $D_s = C_{ps} q_\infty (A_2 - A_1)$. This relationship ($D_s = -D_{1_f}$, or $C_{ps}(A_2 - A_1) = -C_{D1f} A_1$) can be applied to the free-streamline model. If the relationship between C_{D1f} and C_{ps} can be established, (4) will yield an expression for C_{ps} in the model. A suitable relationship can be determined from experimental results as follows.

For isolated discs,

$$C_{D_{1f}} = C_{D1} + C_{ps} \tag{5}$$

where C_{D_1} is the drag coefficient of the disc. An empirical expression for the dependence of C_{D_1} on C_{p_s} may be obtained from measurements of the drag of bodies with cavity wakes collected by Perry & Plesset (1953). The data for discs, for values of C_{p_s} down to −0.25, are well fitted by the expression

$$C_{D_1} = 0.80(1 - C_{p_s}) \tag{6}$$

Thus from (5), $C_{D_{1f}} = 0.80 + 0.20\, C_{p_s}$ which, when substituted in (4), gives for the stream-surface pressure coefficient the result

$$-C_{p_s} = \frac{0.80}{\left(\frac{d_2}{d_1}\right)^2 - 0.80} \tag{7}$$

This semi-empirical result is shown in Fig. 5 (down to values of C_{p_s} as low as −3!) together with the single value determined by Strück from his numerical calculations.

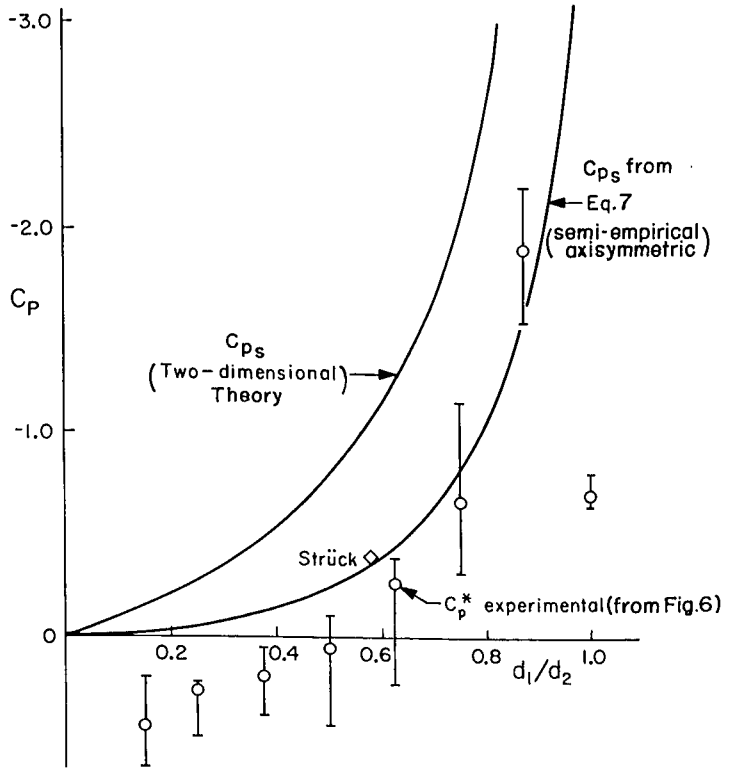

Fig. 5. Optimum-gap pressure.

References p. 273.

In our experiments, the base pressure on the disc was not measured, but pressures in the gap were estimated from pressure distributions measured on the face of the rearbody for optimum configurations, and shown in Fig. 6. Average values of the gap pressure coefficient, C_p*, that were estimated from these distributions are plotted in Fig. 5; they are weighted toward values deeper in the cavity, the excursions near the top being attributed to dynamic effects associated with the reattachment region and with a trapped vortex (these effects are discussed later). The maximum excursions about the selected average values are indicated by the bars in Fig. 5. Again, as in Fig. 4, a rough correspondence between measurements and the free-streamline model is observed. For the optimum axisymmetric test configurations, C_{p_s} of the free-streamline model compares fairly well with the measured average gap pressure. The most notable difference is that in the theoretical model C_{p_s} is always negative, but in the experiment C_p* becomes positive for $d_1/d_2 < 0.5$.

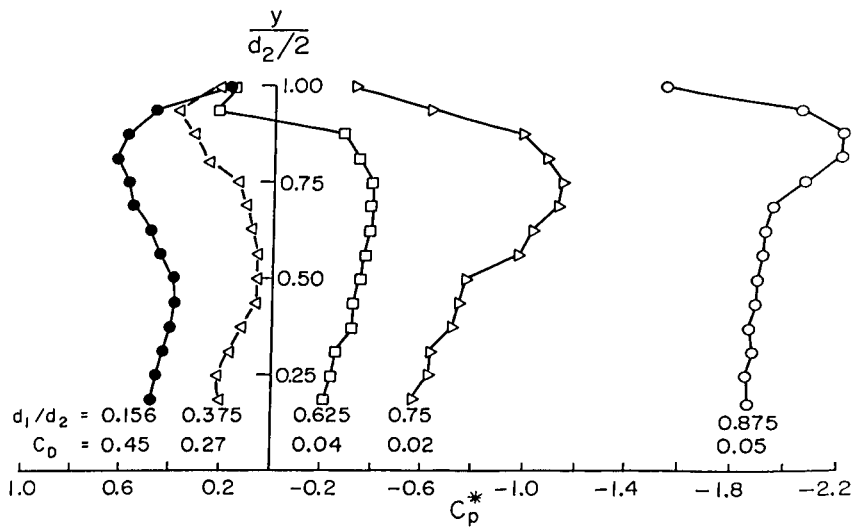

Fig. 6. Pressure distribution on axisymmetric rearbody face at optimum gap.

As a final comparison between theory and experiment, we have attempted to obtain an estimate of the forebody system drag for the optimum geometries. We note that the flow at optimum geometry appears to be a more general example of the flow over a simple gap or cutout in a flat surface with uniform flow over it, and it is constructive to compare the two cases as follows. For the cutout in uniform flow, the free-streamline solution is the simple one, $C_p = 0$ (i.e. $p = p_\infty$) on the streamline spanning the gap and in the gap itself, so that $C_D = 0$. Now the effect of viscous and diffusive effects on the free streamline (which is now the dividing streamline in the free shear layer) is to produce a shear stress along the dividing streamline and a departure from $p = p_\infty$ on the cutout walls. The integral of the perturbed pressure over the walls, together with a small negative contribution from the shear stress on the

bottom, gives the drag of the cutout. A simple momentum balance on the fluid enclosed by the cutout and the dividing streamline shows that the drag

$$D = \int_s \tau_s \, dA_s$$

where the integral is taken over the free surface and τ_s is the shear stress on that surface. Extending this idea to our case of the axisymmetric forebody system, we assume that the shear along the free surface is similarly related to a pressure perturbation $p - p_s$ on the cavity walls (i.e. the front of the rearbody and the back of the frontbody or disc), and we neglect any pressure perturbation on the free surface. Again, a momentum balance gives

$$D = 2\pi \int_s \tau_s r_s \underset{\sim}{n}_x \cdot \underset{\sim}{ds} = 2\pi \int_s \tau_s r_s dx \qquad (8)$$

where $\underset{\sim}{n}_x$ is the direction cosine for the free surface and $\underset{\sim}{ds}$ is a vector element of length along it. The momentum balance properly takes into account the fact that, in the inviscid, free streamline, zero-drag case ($C_p = C_{p_s}$ throughout the gap), the drag on the frontbody, including pressures on its front and back, is just balanced by the negative drag ($C_{p_s} < 0$) on the face of the rearbody.

To evaluate the drag from the integral in (8), we assume that the free shear layer across the gap is a completely developed (self-similar) turbulent flow at constant pressure. For such a flow the value of τ_s is constant on the dividing streamline. The assumption that the path of integration, s, in (8) coincides with the dividing streamline introduces some approximation into the equation, as does the assumption that the value of τ_s is constant all the way to the reattachment point. With these assumptions we use the value which can be determined from the measurements of Liepmann & Laufer (1947), namely, $\tau_s = 0.0115\rho U_s^2$, where U_s corresponds to the flow velocity outside the free shear layer and hence is related to the corresponding pressure coefficient C_{p_s} (which is also $C_p{}^*$ for the gap) by $(U_s/U_\infty)^2 = 1 - C_{p_s}$. Making these substitutions, (8) becomes

$$D = 2\pi (0.0115) \rho U_\infty{}^2 \, (1 - C_{p_s}) \int_{gap} r_s \, dx$$

The integral could be evaluated numerically if the shape of the free stream surface, $r_s(x)$, were available. Instead, we simply use an average value $r_s = \frac{1}{2}(r_1 + r_2)$, which is

References p. 273.

equivalent to assuming that the free stream surface is a truncated cone. With this approximation the result is

$$D = \tfrac{1}{2}\pi(0.0115)\rho U_\infty{}^2 (1 - C_{p_s})(d_2 + d_1)\, g \tag{9a}$$

and

$$C_D = 0.046\left(1 + \frac{d_1}{d_2}\right)(1 - C_{p_s})\frac{g}{d_2} \tag{9b}$$

To obtain C_D as a function of d_1/d_2, we use (7) for C_{p_s} and the two-dimensional free-streamline calculation for g^*/d_2 shown in Fig. 4 since it appears to fit the measurements in the low-drag range. The results are plotted in Fig. 7. Also shown there is one point for which the data from Strück's single numerical axisymmetric calculation were used.

Fig. 7 suggests that our approximations are not unreasonable. For $d_1/d_2 \to 0$, it is clear that $C_D \to \infty$ because, in (9b), $1 - C_{p_s} \to 1$ while $g/d_2 \to \infty$ since the radius of curvature of the separation stream surface varies inversely with C_{p_s}. However, for $d_1/d_2 \to 1$, $1 - C_{p_s} \to \infty$ while $g/d_2 \to 0$ and it is not clear *a priori* what their product will be. For the two-dimensional case, where an exact theory is available, we find $C_D \to \infty$, but for the present calculation $C_D \to 0$.

Whatever the limiting behavior for $d_1/d_2 \to 1$, the agreement of C_D with the magnitude of the experimental values of C_D in the range $0.625 \leq d_1/d_2 \leq 0.825$ is convincing confirmation that in this range the flow over the gap is a simple cavity flow in which the shear layer is the classic turbulent mixing layer. On the other hand for $d_1/d_2 < 0.6$, (i.e. $g^*/d_2 > 0.5$, from Fig. 4) there is a large discrepancy, the measured C_D being much higher than the theoretical value, suggesting a departure from the flow conditions assumed in the model. This is discussed in the following section.

CRITICAL GAP RATIO

For values of g^*/d_2 which are less than about 0.5, i.e. $d_1/d_2 > 0.6$, the flow, as experienced in the wind tunnel and as observed on the flow pictures from the water tunnel, is well behaved. The separation surface is, of course, a turbulent free shear layer, and it appears to develop normally. For larger gaps, however, it becomes unsteady on a larger scale, suggesting some kind of gap-coupled oscillation. For optimum geometries having $g^*/d_2 > 0.5$, the conditions in the turbulent mixing layer are no longer those of a normal layer such as that studied in the Liepmann-Laufer experiment. As may be seen from Figs. 2 and 7, for $d_1/d_2 \geq 0.625$, values of $C_{D\,min}$ are very low, less than 0.05, while for $d_1/d_2 \leq 0.6$ values almost an order of

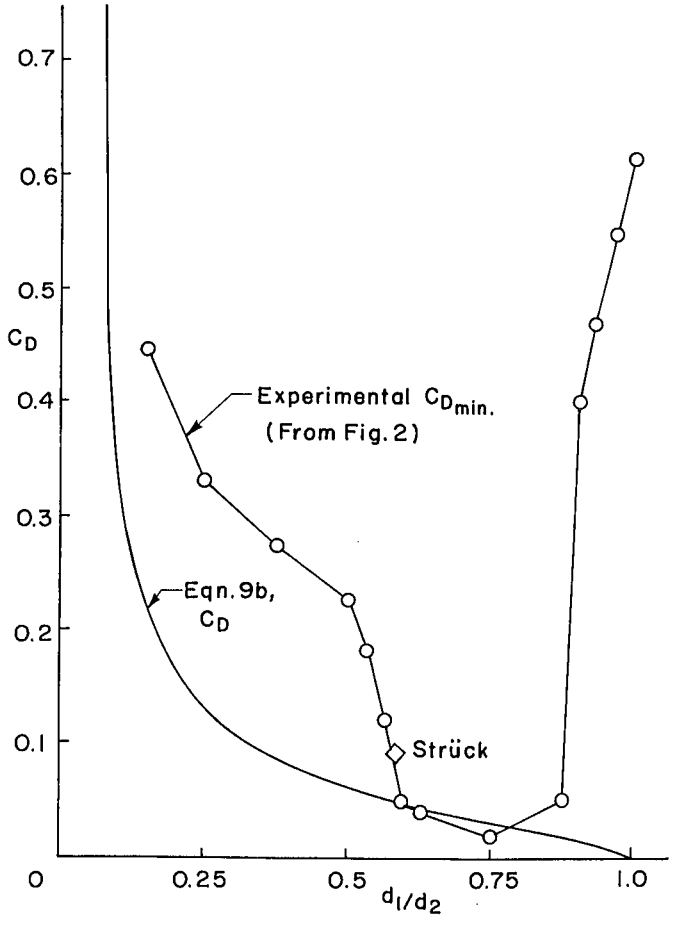

Fig. 7. Comparision of $C_{D\,min}$ and axisymmetric cavity momentum balance.

magnitude higher are attained for optimum configurations. We shall call these the critical values and, temporarily, assign them the values $(d_1/d_2)_{cr} = 0.6$ and $(g^*/d_2)_{cr} = 0.5$. Smaller values of gap ratio will be called subcritical and larger ones supercritical.

Evidence of a critical gap ratio can also be seen in some of the figures previously discussed. For example, it is possible that the critical condition is reached when the gap pressure coefficient passes through zero (Fig. 5); this occurs at $d_1/d_2 = 0.5$ rather than 0.6, but as has been discussed, there is some uncertainty in the correct representative values for gap pressures.

References p. 273.

Also, the pressure distributions in optimum gaps (Fig. 6) show some interesting effects. In particular, the positions of the minima are believed to correspond to the positions of a vortex, which is especially stable and visible in the flow visualizations for subcritical gaps. From Fig. 6 it may be seen that the radial location of this minimum changes rather abruptly at the critical gap (and at $C_p = 0$); the vortex becomes less well-defined, perhaps because of unsteadiness. An interesting observation is that the existence of a steady vortex in the gap is not at all incompatible with low drag and, indeed, may be necessary in some cases.

Also of interest in Fig. 6 is the locus of the pressure maximum, which should correspond to the mean stagnation point of the separation streamline. For subcritical gaps, i.e. the very low values of C_{Dmin}, this position is at or close to the edge of the rearbody face while for supercritical gaps (higher values of C_{Dmin}) it moves some distance inside the edge toward the centerline.

For d_1/d_2 greater than 0.88 the measured values of optimum drag also depart strongly from the values given by (9b). The reason is that the free shear layer does not reattach smoothly because the adverse pressure gradient on the rearbody is now too high.

To conclude this section, there is strong indication of a critical gap ratio below which unusually low values of optimum drag can be achieved. It may be quite useful to consider this behavior when designing for practical applications. The change in flow that occurs for optimum gap ratios larger than critical may correspond to the appearance of a cavity oscillation, but this requires further investigation.

RESULTS FOR SQUARE CROSS-SECTION

Many of the measurements made on the axisymmetric system were repeated for a system with square cross-section, i.e. a box with a square plate in front of it. The question naturally arises whether the same large reductions of drag can be realized as in the axisymmetric case. One might expect the situation to be less favorable since the separation surface leaving the front plate will not retain a square cross-section and so will not reattach smoothly everywhere onto the leading edges of the rearbody. A similar situation would exist in most practical applications. The following figures show the main results.

In Fig. 8 the variation of C_D with g/d_2 is shown for only two values of d_1/d_2, namely 0.25 and 0.75, although measurements were also made for other values. The trends are roughly similar to those for the circular cross-section, with which they are compared in Fig. 8. However, there are some important differences. For the subcritical gap ($d_1/d_2 = 0.75$) the minimum value of C_D is considerably higher than for the circular section, about 0.07 compared to 0.02, although it still represents a full order of magnitude decrease in the drag. That is, in the region where smooth flow

onto the rearbody is crucial, the mismatch between the separated surface and rearbody has a large effect. For the supercritical gap ($d_1/d_2 = 0.25$), there is rather little (percentage) difference between the two cases, suggesting that the mismatch is not so important as for the subcritical gap. This would be consistent with the existence of a large scale oscillation at the supercritical values; that is, one can suppose that a mismatch of amplitude comparable to the amplitude of oscillation of the reattachment point would make little difference.

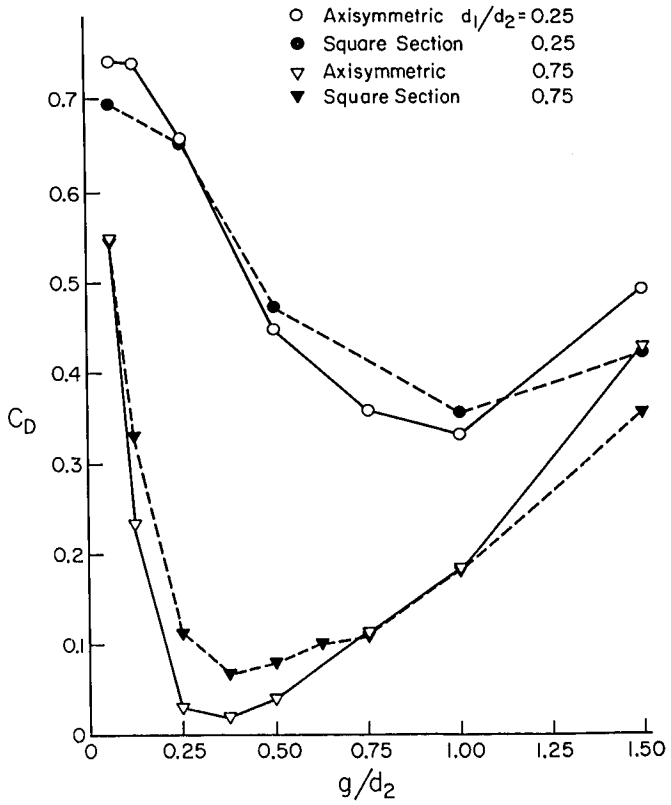

Fig. 8. Effect of cross-section shape.

Side view flow pictures obtained with dye injection are similar to those for the axisymmetric case shown in Fig. 3 and are not included here. More interesting views were obtained by observing the face of the rearbody from an oblique angle. By introducing air into the gap a cavity flow could be created which, while not precisely the same as the fully wetted flow, gave a good impression of the shape of the free

References p. 273.

surface and verified the main features indicated by dye injection in the fully wetted flow. A sketch of the observed flow at an optimum condition (i.e. a minimum value of C_D) is shown in Fig. 9. The most notable feature is the form of that part of the separation surface which springs from a corner of the front plate. In the cavity flow, the wedge-shaped portion of surface is very much like that sketched; it reattaches on the rearbody face inside the corner and is deflected inward. It is probably this reattachment region near the corner that makes the major contribution to the increase in drag as compared to the axisymmetric case, and one might expect some reduction of C_D by cutting away those corners appropriately.

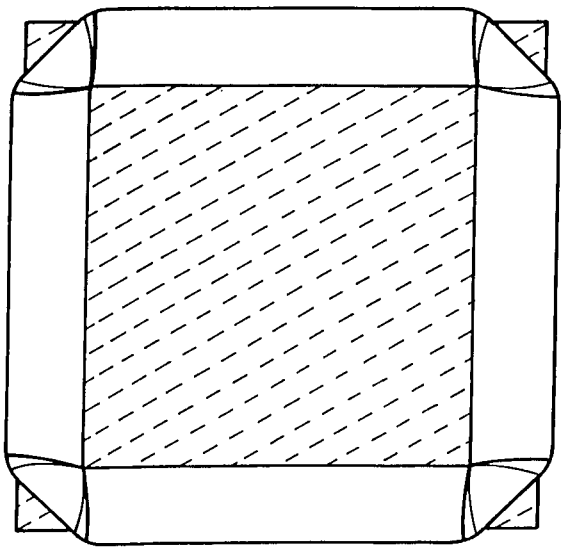

Fig. 9. Front view of cavity separation surface of square cross-section at optimum gap. Cross-hatched areas denote the exposed faces of the front and rearbodies.

ROUNDED CORNERS ON THE AXISYMMETRIC AFTERBODY

The high drag on the rearbody alone could, of course, be drastically reduced, without assistance from a frontbody, by simply rounding its edges sufficiently. A rounding radius equal to one-eighth the body diameter is quite sufficient to reduce the drag of the front face of the rearbody to zero, in the absence of any frontbody, provided the Reynolds number is large enough that premature laminar separation does not occur. In Fig. 10, the rearbody-alone point at $g/d_2 = 0$ and $Re = 500{,}000$ shows the effect of such separation. However, placing a small disc against the face of the rearbody provides sufficient tripping action to avert laminar separation, and the drag coefficient goes to zero.

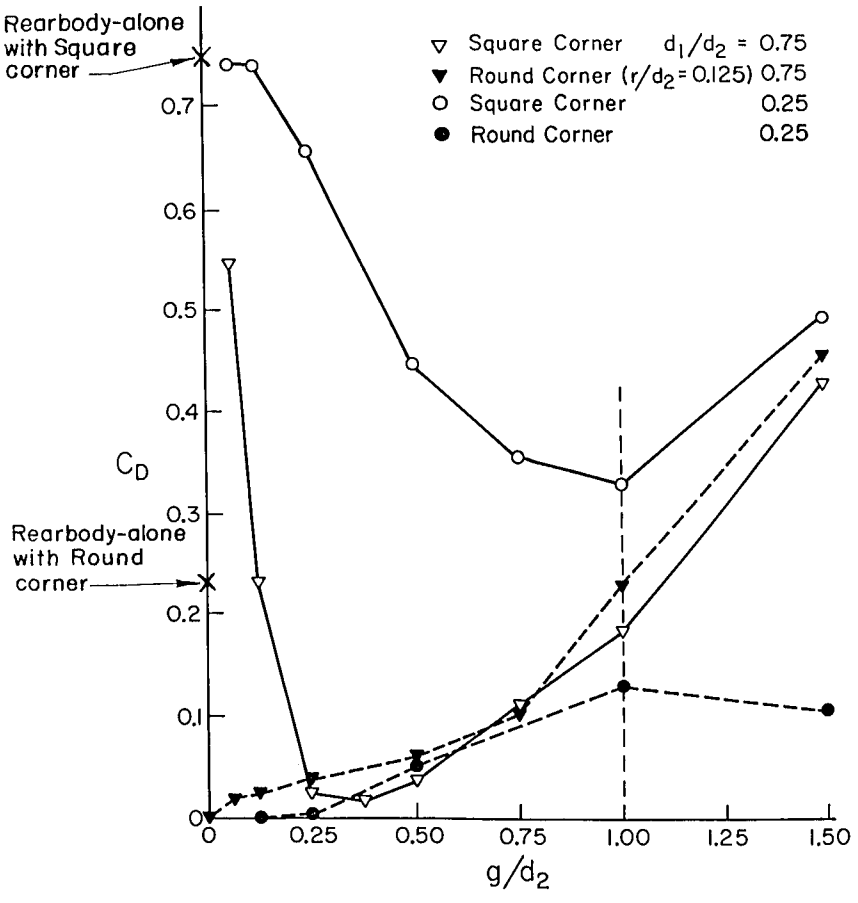

Fig. 10. Effect of corner radius on rearbody.

It is of interest to see what effect a frontbody would have when the rearbody has rounded edges. Some results are shown in Fig. 10 for axisymmetric bodies. Again, the comparison is made for two cases, $d_1/d_2 = 0.75$ and 0.25, respectively, with and without rounded edges. For $d_1/d_2 = 0.75$ and small values of g/d_2 (less than 0.2) rounding of the rearbody results in a very large reduction of drag, because the flow which has reattached onto the face of the rearbody can develop suction on the rounded edges. For large gap ratios ($g/d_2 > 0.2$), on the other hand, the rounding is not helpful. In fact, for intermediate gap ratios, where the square-edged body system has very low drag, rounding of the edges is actually detrimental. For $d_1/d_2 = 0.25$ there is always a very beneficial effect of rounding. This is because the wake of the smaller frontbody is probably already closed at $g/d_2 = 1$ while for the large frontbody ($d_1/d_2 = 0.75$) this development would be delayed to larger values of g/d_2.

References p. 273.

It is clear that for all cases, rounding of the rearbody must be beneficial for $g/d_2 \to \infty$ since it becomes independent of the frontbody. The vertical line drawn at $g/d_2 = 1.00$ refers to the case $d_1/d_2 = 0.25$; it indicates that for gap ratios greater than 1.00, the two bodies are tending to become independent (see eq. 3), with the system drag coefficient tending to the following values:

$$C_D \to 0.75 + 1.2\left(\frac{1}{4}\right)^2 = 0.83\,, \quad \text{square corner}$$

$$C_D \to 0 + 1.2\left(\frac{1}{4}\right)^2 = 0.08\,, \quad \text{rounded corner}$$

For $d_1/d_2 = 0.75$, the asymptotic values are

$$C_D \to 0.75 + 1.2\left(\frac{3}{4}\right)^2 = 1.43\,, \quad \text{square corner}$$

$$C_D \to 0 + 1.2\left(\frac{3}{4}\right)^2 = 0.68\,, \quad \text{rounded corner}$$

A most interesting result of the rounding experiment is that for some gap ratios (subcritical and near optimum) square edges are better than rounded ones. This may be important in those instances where some frontbody is required. A closer investigation of the reattaching flow for these conditions needs to be made, however.

CONCLUDING REMARKS

From these results, it appears that there are three flow regimes for the system with a square-edged rearbody that was investigated: (1) If the shielding frontbody is absent or not optimized, the drag coefficient for the system has the ordinary, bluff-body value of order unity. (2) For a well designed system and for optimum values of gap ratio less than critical, the drag coefficient can be reduced almost two orders of magnitude below bluff-body values. (3) For optimum gap ratios larger than critical, the drag coefficients are of intermediate magnitude.

Although the investigation is not complete, it appears that these changes may be characterized by the scale of the nonsteady motions that occur. In the low drag range (2), the scales of the eddies in the free turbulent shear layer spanning the gap are small, i.e. no larger than about 0.3g, and the eddy motion is independent of the gap geometry; in the intermediate regime (3), fluctuations of larger scale occur, possibly because of a cavity oscillation; in the high drag, bluff-body regime (1), the oscillations are of a scale comparable to the body diameter.

A better understanding of these drag related mechanisms and their relation to the system geometry would be helpful in designing for the substantial drag reductions that appear to be technically feasible.

ACKNOWLEDGEMENTS

The work described here was supported with funds from the Ford-Exxon Energy Research Program of the California Institute of Technology and is being continued under a National Science Foundation Grant. For assistance in the early stages of the research, we are grateful to Professor F. Clauser, who designed and built the force balance for the Merrill Wind Tunnel, and to Mr. R. Breidenthal, who did some early measurements on the drag of a half body. Thanks are also extended to Mr. W. Bettes for various helpful suggestions and to Mr. Till Liepmann for assistance with the experiments.

REFERENCES

Hoerner, S. F. (1965), Fluid-Dynamic Drag, published by the author, Brick Town, N.J.

Liepmann, H. W. & Laufer, J. (1947), Investigations of Free Turbulent Mixing, NACA TN 1257.

Plessel, M. S. & Perry, B. (1954), On the Application of Free Streamline Theory to Cavity Flows, California Institute of Technology.

Roshko, A. (1954), A New Hodograph for Free Streamline Theory, NACA TN 3168.

Roshko, A. (1955), Some Measurements of Flow in a Rectangular Cutout, NACA TN 3488.

Saunders, W. S. (1966), Apparatus for Reducing Linear and Lateral Wind Resistance in a Tractor-Trailer Combination Vehicle., U. S. Patent Office 3, 241, 876.

Strück, H. G. (1970), Discontinuous Flows and Free Streamline Solutions for Axisymmetric Bodies at Zero and Small Angles of Attack, NASA TN D-5634.

Ward, T.M. (1976), The Hydrodynamics Laboratory at the California Institute of Technology, Graduate Aeronautical Laboratories, California Institute of Technology.

DISCUSSION

W. W. Willmarth *(University of Michigan)*

I have some comments about the unsteady flow in the separated shear layer between your front and rearbodies. We did some related work at the University of Michigan involving the development of an open window for an aircraft optical device. And, in talking to Dr. Hucho, it sounds as though there are similar ground vehicle problems with sunroofs. Years ago, when I was at Cal Tech, Karamcheti and Roshko looked at the flow over a cavity and found a tremendous radiation of sound, on the order of 140-160 dB, even at 200-300 ft/sec. What happens is that the shear layer flaps across the back edge of the cavity and pumps air in and out. The ingredients of the problem are the cavity volume, a lot of turbulence, and a very thin shear layer compared to the cavity length.

The first thing we did in trying to solve the problem with our open optical window was to look at a two-dimensional configuration (see Fig. 11). We tried to hop the shear layer over the cavity with a small, upstream ramp so that reattachment definitely occurred downstream of the rear edge. That cut the sound radiation quite a bit, but not entirely. At that point we hadn't done anything about the thin shear

layer, so we took a crack at that. Practically, it wasn't feasible to increase the upstream body length to get a thicker boundary layer, so we came up with the scheme of using a series of high drag, porous fences just upstream of the cavity. The fences

W. W. Willmarth

had to be porous. We tried all combinations, but the best seemed to be with the biggest one first and the next ones succeedingly smaller in a linear fashion. Three or four are all you need. As I see it, the idea was to make some big eddies with the leading fence and then chop them up by having the flow go through and around the smaller screens. The shear layer over the cavity becomes very thick and, as a result, the reattachment is reasonably steady, velocities in the cavity are quite low, and you can kill the resonance.

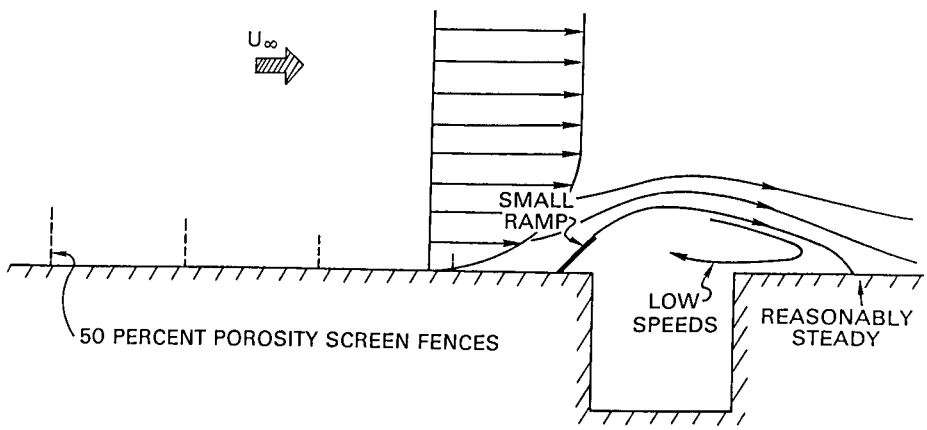

Fig. 11. Control of flow over a two-dimensional cavity using porous fences and a ramp.

The final configuration of the optical device (see Fig. 12) was axially symmetric and more complicated than our two-dimensional configuration. It also had to be insensitive to angle of attack over a range of ±12 degrees at speeds of 100 to 200 m/s. We measured the pressure in the cavity as a function of time, and the odd thing we

found was that the smallest fluctuations occurred at a tilt of about 4 degrees rather than at an angle of zero. The rms pressure in the cavity was comparable to that found on the wall beneath a flat plate turbulent boundary layer; the rms velocity was only 0.006 U_∞ with maximum fluctuations of only 0.04 U_∞. It was really quiet. The solution to the cavity problem we worked out here might work on any cavity where you have a very short run upstream of the separated shear layer.

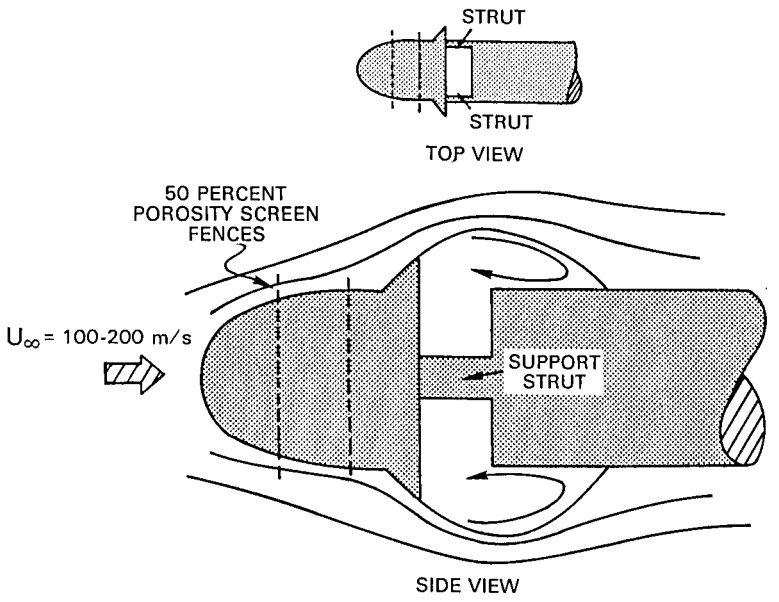

Fig. 12. Practical application of fences and ramp to control flow over a cavity in an axially symmetric body. Additional side support strut detail is shown in smaller top view sketch.

A. Roshko

I think that's a nice piece of work and very relevant to our two-body problem. It seems quite likely to me that a changeover from a highly oscillating to a very quiet cavity flow may correspond to what we called our critical gap length. I would interpret your results as follows, which is, I think, basically the way you looked at it. If you have a free shear layer, even though it's turbulent, you can think of that layer as having an instability problem itself. That is, it might build up large oscillations. The distance required to build up such oscillations is measured in terms of the initial thickness of the layer. I would think that thickening the boundary layer increases the distance required for a large oscillation to build up, and that's perhaps what solved your problem. Similarly, in terms of our critical gap, it would seem that by increasing the boundary layer thickness ahead of the gap, you could extend the critical gap length to a larger value. That's certainly something we'll want to try.

R. T. Jones *(NASA-Ames Research Center)*

Don't you think you could suppress the cavity oscillation by putting a screen just inside the cavity, parallel to the mean flow? I'm sure that if you put a little screen inside the mouth hole of a flute, the player would never be able to make a sound. So you shouldn't need things like fences and ramps on the *outside*, just some damping of the motion *inside*.

W. W. Willmarth

I think the key thing with our oscillating cavity flow *and* with Roshko & Koenig's supercritical and subcritical gap ratios, is the pumping action of the thin shear layer as it leaves the upstream edge of the cavity. If you can do something upstream that will reduce the gradient of the shear, then there will be much less entrainment or pumping. It's the pumping that sucks the cavity down to low pressures and starts the oscillation.

D. J. Maull *(Cambridge University, England)*

I have a comment on Professor Willmarth's work. The cavity problem has been looked at almost ad nauseum, starting with the problem of bomb bay buffeting. His precise problem was almost completely cured by rounding the downstream edge of the bomb bay cavity. I think it makes sense, intuitively, that flows don't like to reattach, nor do humans, on sharp corners. I think it would be better to treat the downstream edge of the cavity rather than trying to modify the approach flow.

D. J. Maull

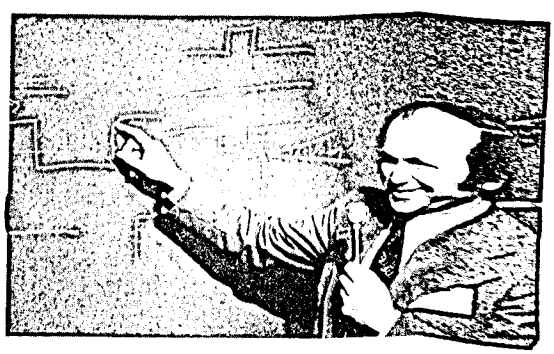

A. Roshko

A. Roshko

I don't think you can always depend on treating the downstream edge. There's a remarkable counter-example that we saw in the case of supersonic flow over a cavity. With a square downstream corner the flow was rather quiet – there was very weak external radiation of noise. However, when we rounded that corner, which we hoped

would even further reduce the radiated noise, we got an incredible whistling – a very strong external noise radiation.*

R. Sedney *(U.S. Army Ballistic Research Laboratories)*

I have another addition to Professor Willmarth's work. About eight years ago we worked on the same problem at the Martin Company. The solution was a ramp which came up at about 45 degrees and bled off about 1/4 of the boundary layer (see Fig. 13). There was a porous plate at the downstream end of the ramp. It was a tremendously efficient solution for cutting down cavity oscillation and external noise radiation.

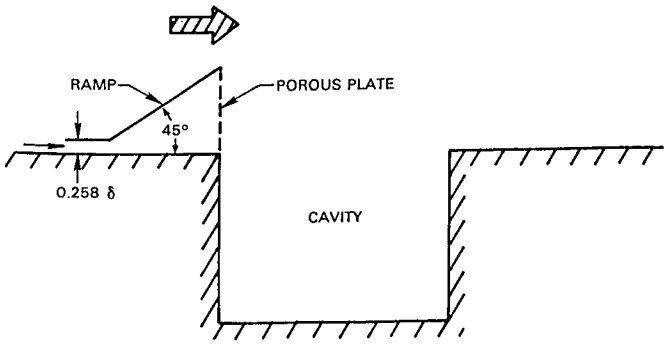

Fig. 13. Combination of ramp, boundary layer bleed, and porous fence to control flow over a cavity.

P.B.S. Lissaman *(Aerovironment, Inc.)*

We've developed a porous air deflector for trucks that seems to exhibit some of the features that have been discussed in conjunction with these cavity flows. Because of our deflector's intentionally selected porosity, the buffeting transmitted to the tractor is enormously reduced. It also seems to work very well in cross winds, and we believe this has something to do with the small scale of turbulence coming through the perforated screen, as well as with the lip-like protrusions provided on its side edges.

R. T. Jones

In all this discussion of the gap flow details have we forgotten that one of the main points of your paper is that you succeeded in *eliminating* the drag of the forebody?

*Thomke, G. (1964), *Separation and Reattachment of a Turbulent Boundary Layer Behind Downstream Facing Steps and Cavities, Douglas Aircraft Company Report SM-43062.*

A. Roshko

I think the questions connected with the critical gap are perhaps pertinent in trying to understand the mechanism that destroyed the very low drag levels at subcritical gaps.

R. T. Jones

Since your test body was semi-infinite, its drag did not include that of the base. What final drag coefficient can you predict for us if you include the base drag?

A. Roshko

The base drag coefficient for one of these bodies is about 0.2. Since the forebody drag would be zero, the total drag would also be 0.2.

R. T. Jones

This would be the minimum total drag at zero yaw angle. Crosswinds would create non-zero yaw angles. Wouldn't you have to also put dams in somewhere else to prevent a mismatch between the gap shear layer and the leading edges of the rearbody?

A. Roshko

I think you might have to have *adjustable* flaps, or dams, on the frontbody if you really wanted to do it right, that is to *always* guide the flow precisely onto the leading edges of the rearbody at all angles of yaw. It would get rather complex.

H. H. Korst *(University of Illinois)*

Why have you chosen the dissipation integral from minus ∞ to plus ∞ as the significant force contribution? It would appear that it might be a good idea to use the momentum integral from minus ∞ to the reattaching streamline instead. Did you try that?

A. Roshko

No, we did not. That would be another way to do it. In fact, with the momentum integral it is easier to keep the various terms under control, because in applying the dissipation integral to the gap flow you really are neglecting some dissipation which is occurring farther downstream.

Editors' Comment: In preparing their paper for publication in the Proceedings

Roshko & Koenig did in fact reformulate their calculations according to a momentum balance.

H. H. Korst

My second question concerns the hodograph theory. You probably considered the change in the pressure distribution on the front face of the plate in the sense of Jakob. When Jakob, in 1926, started the modification of the free streamline theory with parametric pressures in the wake, he also found a modification of the pressure distribution on the front face of 2-D plates. That provided a very attractive way of obtaining simple things, such as plate drag, in a more realistic manner. If you take the actual pressure distribution that results from such a parametric definition of the free streamline, you come up with values that are quite close to those we expect from experiment, instead of the high values that you get. Have you considered that in advance?

A. Roshko

Jakob's method, or that of Parkinson & Jandali which is pretty much the same thing, or other free streamline methods, all have the base pressure as a parameter. My impression for something like a plate or a disk is that once you have chosen the base pressure coefficient, that fixes the pressure at the edges of the plate or the disk, and also the pressure distribution over the whole front face of the body. So the force calculated from the method comes out very accurately. So, I don't think that this is going to produce very much difference.

D. J. Maull

Several years ago we had a look at the inverse of Roshko & Koenig's problem – a cavity in an axisymmetric pipe. The reason we were looking at the axisymmetric case was that when we had first tried a two-dimensional cavity, the flow broke down into cells across the width of the cavity. Unfortunately, we found that the axisymmetric case also broke down into cells. These rotated very slowly around the cavity, unless they were fixed in circumferential position by a small, local asymmetry in the cavity geometry. Did you find any cellular structures in your cavities?

A. Roshko

I must admit that we haven't looked at it closely enough to notice. But I think it's interesting to know that a cellular breakdown in a two-dimensional cavity might actually correspond to a circumferential instability.

S. Saunders *(Rudkin-Wiley Corporation)*

Professor Roshko has attributed to me a great deal more understanding of the